NCCPM
National Co-ordinating Centre for the Physics of Mammography

Technical evaluation of contrast enhanced mammography functions of GE Essential system

Technical Report 2001

January 2020

Alistair Mackenzie, Nicola Tyler, Mary Kelly

Acknowledgements

The authors are grateful to the staff at the Addenbrookes Hospital, Cambridge, for their assistance with the evaluation of this equipment.

Funding

This study was funded for the NHS Breast Screening Programme by Public Health England.

Contents

1. Introduction

1.1 Evaluation report

At the time of publication of this report, the use of contrast enhanced mammography (CEM) systems is not approved for use in the NHS Breast Screening Programme (NHSBSP). Currently, the technology is being evaluated clinically. Further updates on approvals can be found on the PHE website: https://www.gov.uk/government/publications/breast-screening-status-of-approved-equipment.

This report is one of a series evaluating the use of CEM on commercially available mammography systems and comprises a summary of the performance of CEM. There is currently no NHSBSP guidance on testing of CEM systems. The methodology developed for this evaluation was primarily based on work by Oduko et al.[1,2] The GE Essential full field digital mammography system was previously evaluated.[3]

1.2 Objectives

The purpose of the evaluation was to assess the performance of the GE software for CEM of the GE Essential mammography system (SenoBright).

1.3 Contrast enhanced mammography description

CEM involves the administration of an iodinated contrast agent to the woman. Two images are acquired in close succession following administration; the first at a low energy and the second at a higher energy. These exposures are designed to have the majority of the energy of the spectra of the two exposures above and below the K-edge of iodine. An algorithm is then applied to create an image without breast structure and showing the location of any iodine accumulation. The accumulation of iodine is a potential indicator of a cancer.

2. Methods

The following describes the standard method for testing the CEM functions. Any system specific testing methods will be described in the results.

2.1 System tested

The system tested is described in Table 1.

Table 1. System description

Location	Addenbrooke's Hospital, Cambridge
Manufacturer	GE Medical
Model	Essential
System Serial Number	2079155118122
Anode target material	Rhodium (Rh), Molybdenum (Mo)
Additional filtration	0.025 mm Rh, 0.030 mm Mo, 0.3 mm Copper (Cu) & 0.3 mm Aluminium (Al)
Detector type	Caesium Iodide
Detector model	Apollo LFOV
Detector size	Active imaging area not less than 239 mm x 306 mm
Pixel pitch	100 µm
Detector serial number	PLC0108_02
Software version	ADS_55.20

2.2 Phantoms

CEM phantom

A phantom designed by Leithner et al[4] was used in the evaluation. The phantom consists of a 300 x 240 x 20 mm^3 PMMA block. Embedded within the phantom are 5 mm diameter discs containing Iopamidol at concentrations ranging from 0.25 to 2 mg cm^{-2} of iodine. Discs containing 0 mg cm^2 iodine are also included in the phantom, as well as air-filled discs. Figure 1 shows an example subtracted image of the phantom whilst Figure 2 shows the composition of each disc within the matrix of 8 columns and 5 rows.

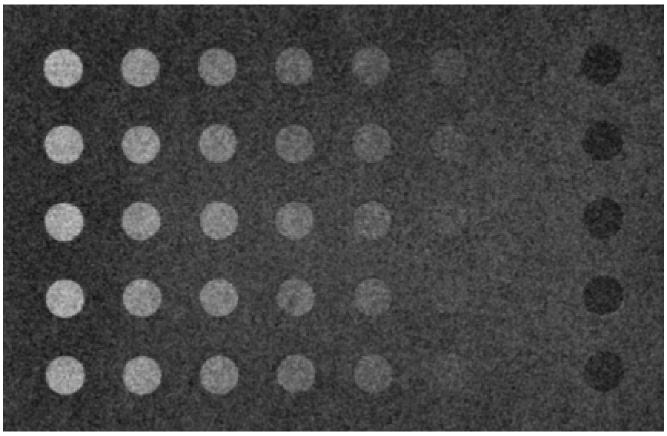

Figure 1. Central region of subtracted image of CEM phantom

2	1.5	1	0.75	0.5	0.25	0	Air
2	1.5	1	0.75	0.5	0.25	0	Air
2	1.5	1	0.75	0.5	0.25	0	Air
2	1.5	1	0.75	0.5	0.25	0	Air
2	1.5	1	0.75	0.5	0.25	0	Air

Figure 2. Iodine concentration of each disc in CEM phantom in terms of mg cm^{-2}. Discs in final column comprised of air.

Tissue equivalent blocks

The majority of the tests were undertaken using tissue equivalent blocks produced by CIRS (Norfolk, VA, USA). These blocks are designed to have similar attenuation properties as for specific fibroglandular densities of breast tissue. Dance *et al*[5] described model to be used in breast dosimetry for a range of thicknesses from 20 to 110 mm. The model includes two 5 mm thick layers of fat at the upper and lower surface of the breast as well as an expected glandularity for the central portion of the breast. CIRS blocks of different densities by mass were selected to match as closely as possible those densities, in addition to the use of 5 mm of CIRS fat blocks at the bottom and top of the stack. Tables 2 and 3 show the thickness of blocks used to simulate the different thicknesses with and without the CEM phantom. Overall, a good match in density was found between the required glandularity and the actual value.

Table 2. Thickness of blocks of CIRS tissue equivalent material used for different phantom thicknesses including 2 x 5 mm thick fat

Total phantom thickness (mm)	Target glandularity of central area (%)	Glandularity of central portion (%)	CIRS Phantom [percentage glandularity is stated] (mm)				
			Fat [0%]	30:70 [30%]	50:50 [50%]	70:30 [70%]	Glandular [100%]
20	100	100%					10
30	72	70%				20	
40	50	50%			30		
50	33	33%	10	20		10	
60	21	21%	30	10		10	
70	12	12%	50			10	
80	7	7%	60		10		
90	4	4%	70	10			

Table 3. CEM phantom plus thickness of blocks of CIRS tissue equivalent material used for different phantom thicknesses

Total phantom thickness (mm)	Target glandularity of central area (%)	Glandularity of central portion (%)	CIRS Phantom [percentage glandularity is stated] (mm)				
			Fat [0%]	30:70 [30%]	50:50 [50%]	70:30 [70%]	Glandular [100%]
30	72	76%			10		
40	50	52%	10		10		
50	33	34%	20	10			
60	21	22%	40				
70	12	18%	50				

2.3 Output and HVL

The output and half-value-layer (HVL) were measured as described in the NHSBSP protocol,[6] at intervals of 3 kV or, if only a limited number of options are used clinically, then only those options were measured.

2.4 Detector performance

Testing was carried out using 50 mm thick tissue equivalent material at the X-ray tube port and with the anti-scatter grid in position (Table 2). The beam was collimated to approximately 100 × 100 mm^2 at the detector housing. The mean pixel value (PV) was measured in a region of interest of 5 × 5 mm^2 within the irradiated area. The relationship between mean PV against mAs was then determined.

2.5 Uniformity and artefacts

A uniform block of PMMA was placed on the breast support and imaged under automatic exposure control (AEC) in contrast enhanced mode. Generally the block supplied by the manufacturer for flat fielding was used. The mean pixel values of 5 × 5 mm^2 ROIs were measured in nine locations across the image. The variation in signal across the image was then calculated. The image was viewed using a narrow window to examine any artefacts that may adversely affect clinical image quality.

2.6 Automatic exposure control repeatability

The CEM phantom was imaged with 30 mm thick breast equivalent tissue blocks (Table 3) for a total thickness of 50 mm. The phantom was imaged under AEC in contrast enhanced mode. This was repeated until five sets of images were acquired.

Subtracted images were analysed to calculate the Signal Difference (SD), i.e. the difference in pixel value between the each iodine disc and the background region. The contrast-to-noise ratio

(CNR) for each disc was calculated by dividing the SD by the root mean square of the standard deviation in the iodine disc and background region. The SDs and CNRs quoted in this report are the mean values for the five identical discs of each iodine concentration.

2.7 Variation in AEC Performance and Image Quality with Phantom Thickness

The CEM phantom was imaged under AEC with varying combinations of tissue equivalent blocks, as shown in Table 3. Images were analysed to determine the SD and CNR for each iodine concentration.

2.8 Mean glandular dose

Exposures were carried out under AEC using the combinations of tissue equivalent blocks specified in Table 2. The exposure factors were noted and mean glandular doses (MGDs) were calculated for equivalent breast thicknesses using standard methods by Dance et al.[5,7]

2.9 Comparison of MGD between Low Energy CEM and Standard 2D Images

Images were acquired of the tissue equivalent blocks listed in Table 2 in standard 2D mode using AEC. These values were then compared with the low energy exposure of the contrast enhanced exposures.

2.10 Subtraction with background

CIRS BR3D phantom slabs (Figure 3) were used to assess whether the system was capable of subtracting the tissue-like structures from images to reveal a spot of iodine placed between the slabs.

Figure 3. CIRS BR3D phantom

3. Results

3.1 X-ray tube output and half value layer

The output and half value layer for the system in high energy mode is shown in Table 4.

Table 4. X-ray tube standard output measurements for high energy CEM image exposure parameters

kV, Target/Filter	Tube Output (μGy/mAs @ 100 cm)	HVL (mm Aluminium)
45 kV Mo/Cu	1.09	3.24
46 kV Mo/Cu	1.25	3.24
45 kV Rh/Cu	1.21	3.27
47 kV Rh/Cu	1.52	3.42
49 kV Rh/Cu	1.87	3.55

3.2 Detector Performance

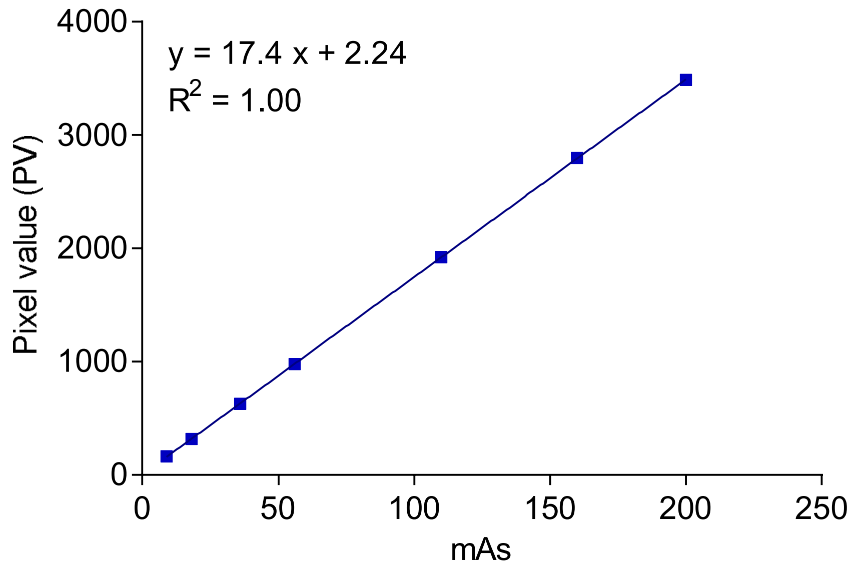

Figure 4. Variation in pixel value of high energy CEM image with mAs

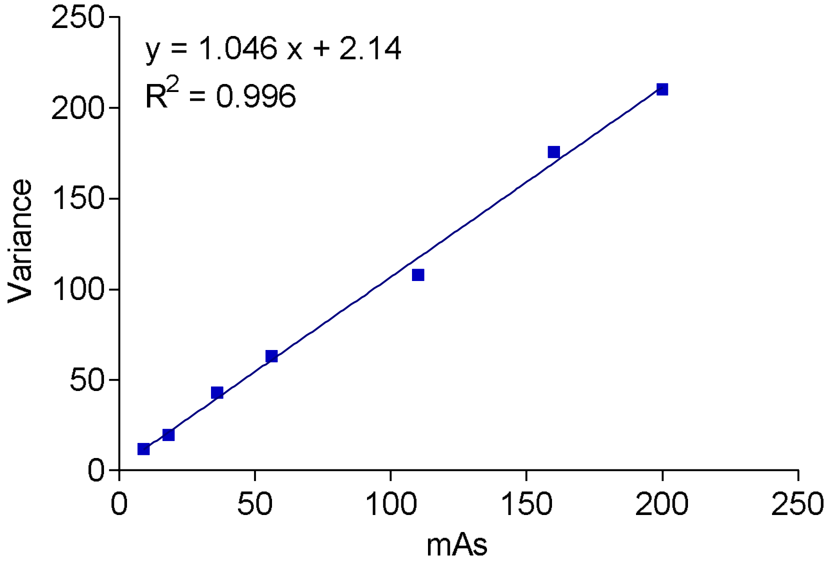

Figure 5. Variation in high energy CEM image variance with mAs

The exposures were acquired using 45 kV and a Rh/Cu target/filter combination. Figures 4 and 5 demonstrate that pixel value and variance (standard deviation squared) are linear with mAs (and hence detector dose) over this range of mAs values.

3.3 Uniformity and artefacts

The uniformity measurement was undertaken using the 25 mm thick PMMA block provided by GE for the flat field calibration of this system. Percentage non-uniformity was measured using unprocessed low and high energy images. The maximum variation in pixel value from the centre of the image was 1.6% and 1.1% for the low and high energy images respectively. Both values are below the NHSBSP remedial level of 10%.

Artefact evaluation was performed on low and high energy images as well as subtracted images. Only a faint ghosting artefact was seen on the unprocessed images, which is expected for this type of detector.

3.4 Repeatability of exposures under AEC

The AEC repeatability test was performed using a 50 mm thick phantom comprised of 20 mm CESM phantom with added tissue equivalent material. The repeatability was within tolerance and the results are shown in Table 5.

Table 5. Repeatability of mAs, SD and CNR for CEM exposures for 1.0 mg cm^{-2}

Max % variation from mean mAs	Low energy CEM exposure	0%
	High energy CEM exposure	0%
Max % variation from mean SD		2.8%
Max % variation from mean CNR		3.4%

3.5 Variation in AEC Performance and Image Quality with Phantom Thickness

The CEM phantom was imaged with blocks of breast equivalent tissue as shown in Table 3. The results for 1.0 mg cm^{-2} iodine are shown in Table 6. The results for the other concentrations are shown in figures 6 and 7. For all iodine concentrations, the SD tends to decrease with increasing phantom thickness when imaged in AEC mode (Figure 6); however the CNR remains relatively constant (Figure 7). The SD and CNR increase linearly with iodine concentration for any given phantom thickness (Figures 8 and 9).

Table 6. Variation in exposure parameters, SD and CNR for CEM subtracted images acquired in AEC mode for 1.0 mg cm^{-2}

Phantom thickness (mm)	kV Target/Filter		SD	CNR
	Low energy exposure	High energy exposure		
30	27 Mo/Rh	46 Mo/Cu	40.2	2.95
40	28 Mo/Rh	45 Mo/Cu	38.4	2.92
50	29 Rh/Rh	45 Rh/Cu	36.3	3.05
60	31 Rh/Rh	49 Rh/Cu	36.4	3.29
70	30 Rh/Rh	49 Rh/Cu	35.5	3.18

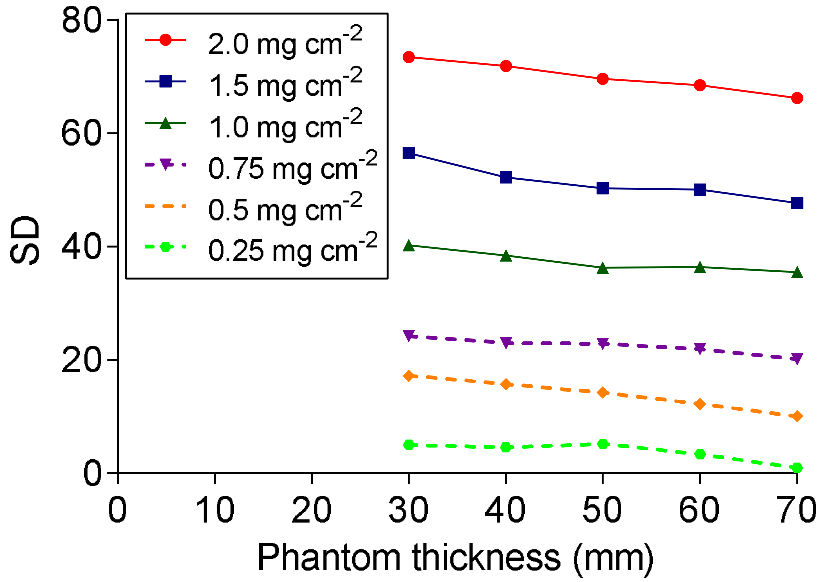

Figure 6. SD with varying phantom thickness for different concentrations of iodine (mg cm^{-2})

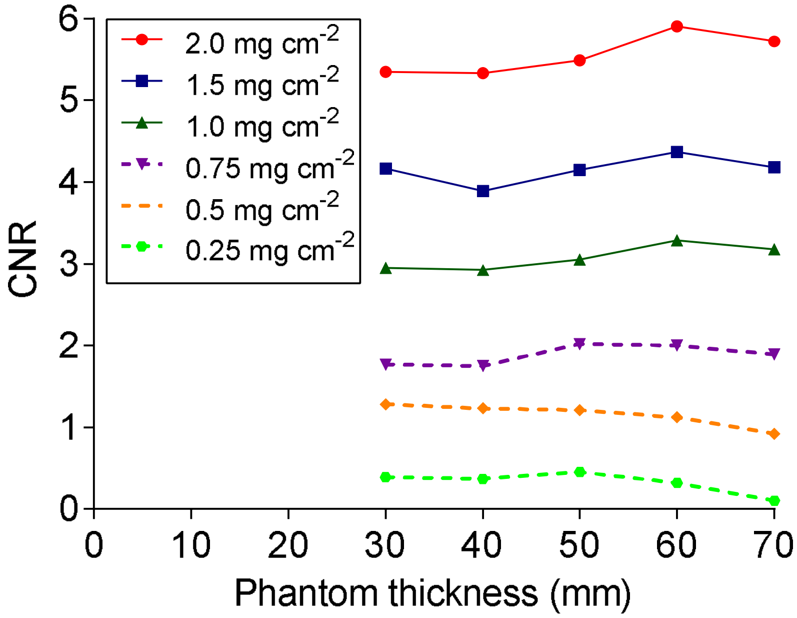

Figure 7. CNR with varying phantom thickness for different concentrations of iodine (mg cm^{-2})

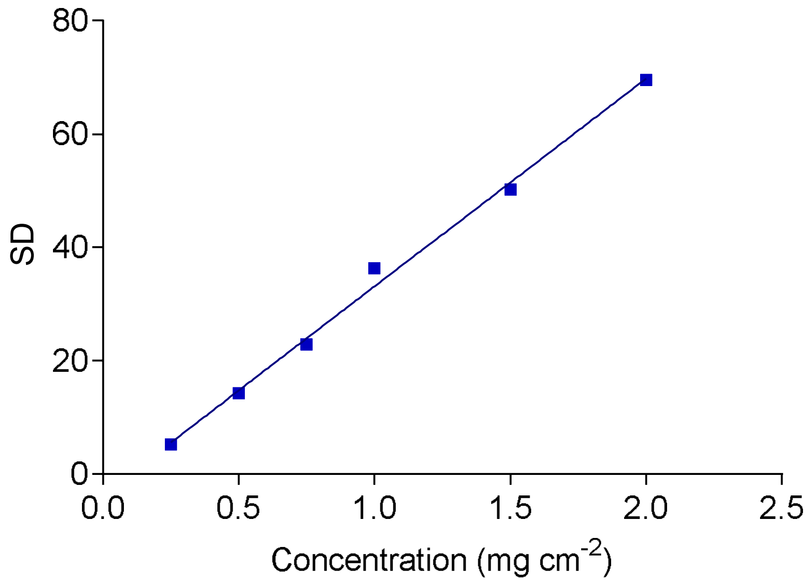

Figure 8. SD with varying iodine concentration for 50 mm thick phantom

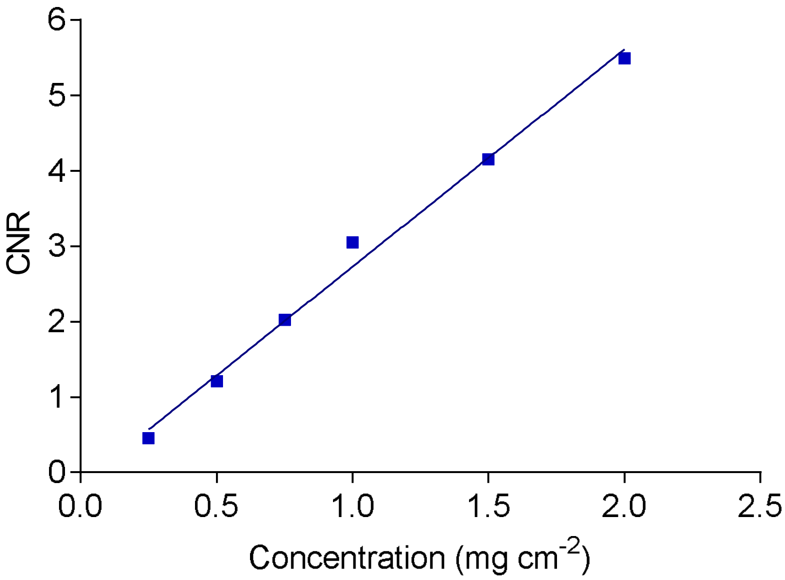

Figure 9. CNR with varying iodine concentration for 50 mm thick phantom thickness

3.6. Mean Glandular Dose (MGD)

The MGD for the tissue equivalent blocks with and without the CESM phantom are shown in Table 7 and Table 8 respectively. The value of *s* used in the calculation of MGD for the Mo/Cu and Rh/Cu target filter combinations was 1.0.

Table 7. MGDs for exposures carried out using CESM phantom with additional tissue equivalent material

Phantom thickness (mm)	Glandularity	Exposure parameters (kV Target/Filter)		Calculated MGD (mGy)		
		Low energy exposure	High energy exposure	Low energy exposure	High energy exposure	Total
30	76%	27 kV, Mo/Rh, 40.4 mAs	46 kV, Mo/Cu, 78 mAs	1.00	0.26	1.26
40	52%	28 kV, Mo/Rh, 63.7 mAs	45 kV, Mo/Cu, 120 mAs	1.53	0.34	1.87
50	34%	29 kV, Rh/Rh, 63.2 mAs	45 kV, Rh/Cu, 176 mAs	1.50	0.53	2.04
60	22%	31 kV, Rh/Rh, 71.2 mAs	49 kV, Rh/Cu, 198 mAs	1.98	0.92	2.90
70	18%	30 kV, Rh/Rh, 125.4 mAs	49 kV, Rh/Cu, 198 mAs	2.85	0.90	3.75

Table 8. MGDs for exposures carried out using tissue equivalent material only

Phantom thickness (mm)	Glandularity	Exposure parameters (kV Target/Filter)		Calculated MGD (mGy)		
		Low energy exposure	High energy exposure	Low energy exposure	High energy exposure	Total
20	100%	27 kV, Mo/Rh, 40.4 mAs	46 kV, Mo/Cu, 78 mAs	1.29	0.27	1.56
30	70%	27 kV, Mo/Rh, 40.4 mAs	46 kV, Mo/Cu, 78 mAs	1.00	0.26	1.26
40	50%	28 kV, Mo/Rh, 63.7 mAs	45 kV, Mo/Cu, 120 mAs	1.53	0.34	1.87
50	33%	29 kV, Rh/Rh, 63.2 mAs	45 kV, Rh/Cu, 176 mAs	1.50	0.54	2.04
60	21%	31 kV, Rh/Rh, 71.2 mAs	47 kV, Rh/Cu, 198 mAs	1.98	0.74	2.72
70	12%	30 kV, Rh/Rh, 125.4 mAs	49 kV, Rh/Cu, 198 mAs	2.85	0.90	3.75
80	7%	30 kV, Rh/Rh, 125.4 mAs	49 kV, Rh/Cu, 198 mAs	2.64	0.87	3.50
90	4%	30 kV, Rh/Rh, 125.4 mAs	49 kV, Rh/Cu, 198 mAs	2.45	0.84	3.29

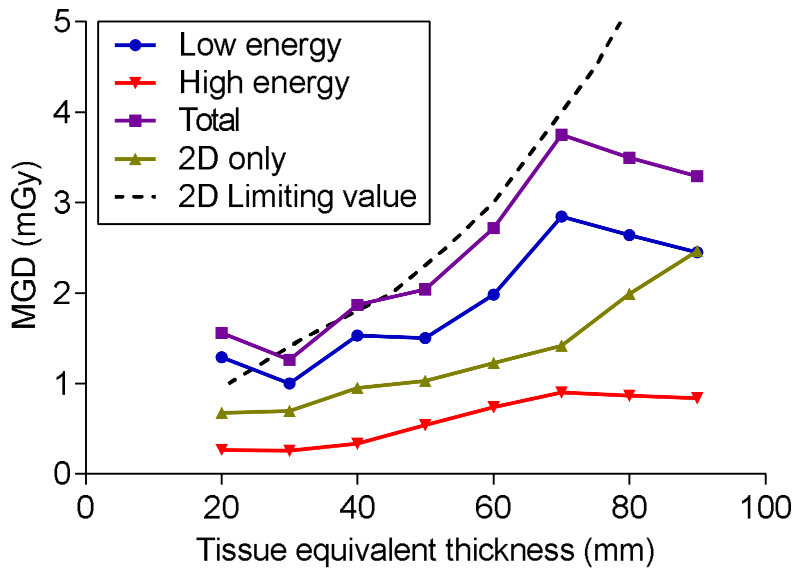

Figure 10. MGD for tissue equivalent material

The radiographic exposure factors of CEM became fixed for the low energy exposure image thin and thick breasts. The minimum factors were 27kV, Mo/Rh, 40mAs and these were selected for 30mm CBT and below. The maximum factors were 30kV, Rh/Rh, 125mAs and were selected for 70mm CBT and above. For reference, the MGDs for 2D full field digital mammography using STD AOP mode AEC were also calculated.

The MGD for tissue equivalent material is shown in Figure 10. This is a different imaging modality from 2D imaging and so the limiting dose values are not relevant, but it is of interest to compare them. It can be seen that the calculated MGD is above the limiting dose values for 2D screening for the 20 mm thick blocks. The higher value of MGD at 20 mm and the decreasing MGD above 70 mm CBT are due to the limitation of factors described in the previous paragraph.

3.7. Accuracy of Indicated MGD

Table 9. Accuracy of indicated MGD

Phantom thickness (mm)	MGD (mGy) for low energy exposure			MGD (mGy) for high energy exposure			% error for total MGD
	Calculated	Indicated	% error	Calculated	Indicated	% error	
20	1.29	1.09	-15.4	0.27	0.22	-17.5	-15.8
30	1.00	0.93	-7.0	0.26	0.22	-14.9	-8.6
40	1.53	1.48	-3.6	0.34	0.29	-14.1	-5.5
50	1.50	1.47	-2.1	0.53	0.44	-17.7	-6.2
60	1.98	1.97	-0.5	0.74	0.64	-13.5	-4.1
70	2.85	2.86	0.2	0.90	0.83	-7.3	-1.6
80	2.64	2.68	1.6	0.86	0.8	-7.5	-0.6
90	2.45	2.63	7.4	0.84	0.77	-8.0	3.5

Table 9 shows the difference between the calculated MGD and MGD shown by the system. The maximum difference between the two MGDs was 15.4% for the low energy exposure and 17.5% for the high energy exposure, with a maximum error of 15.8% for the total MGD.

3.8. Comparison of MGD between Low Energy CEM and Standard 2D Images

Exposure parameters (kV and filter) were different between low energy CEM exposures and standard 2D exposures for the same test object, as shown in Table 10. The MGD of the CEM low energy exposure was generally larger than of the standard 2D images, except 90 mm CBT.

Table 10. Variation in exposure parameters for low energy CEM and standard 2D exposures in AEC mode

Compressed Breast Thickness (mm)	kV Target Filter, mAs, MGD	
	CEM low energy exposure	Standard 2D exposure
20	27 kV, Mo/Rh, 40.4 mAs, 1.29 mGy	25 kV, Mo/Mo, 27 mAs, 0.68 mGy
30	27 kV, Mo/Rh, 40.4 mAs, 1.00 mGy	26 kV, Mo/Rh, 33 mAs, 0.70 mGy
40	28 kV, Mo/Rh, 63.7 mAs, 1.53 mGy	27 kV, Mo/Rh, 45.2 mAs, 0.95 mGy
50	29 kV, Rh/Rh, 63.2 mAs, 1.50 mGy	29 kV, Rh/Rh, 43.4 mAs, 1.03 mGy
60	31 kV, Rh/Rh, 71.2 mAs, 1.98 mGy	29 kV, Rh/Rh, 57 mAs, 1.23 mGy
70	30 kV, Rh/Rh, 125.4 mAs, 2.85 mGy	29 kV, Rh/Rh, 70.9 mAs, 1.42 mGy
80	30 kV, Rh/Rh, 125.4 mAs, 2.64 mGy	30 kV, Rh/Rh, 94.5 mAs, 1.99 mGy
90	30 kV, Rh/Rh, 125.4 mAs, 2.45 mGy	31 kV, Rh/Rh, 112.6 mAs, 2.47 mGy

3.9 Subtraction of BR3D Tissue-Equivalent Material

A small sample of iodine was imaged with the tissue-equivalent, heterogeneous material (CIRS BR3D phantom slabs) to assess whether the system could successfully subtract the swirling, tissue-like structures (as seen in Figure 11) to reveal the iodine sample. Figure 12 demonstrates the successful subtraction.

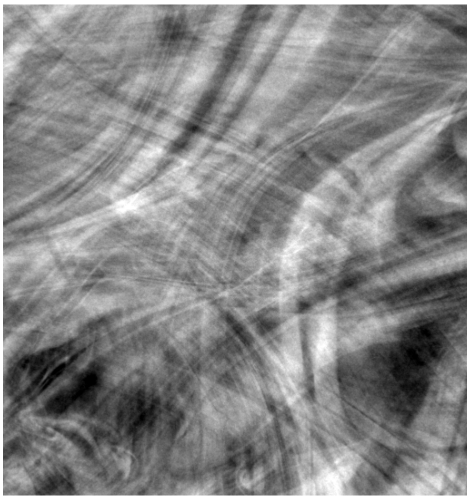

Figure 11. Low energy image of iodine sample with BR3D material

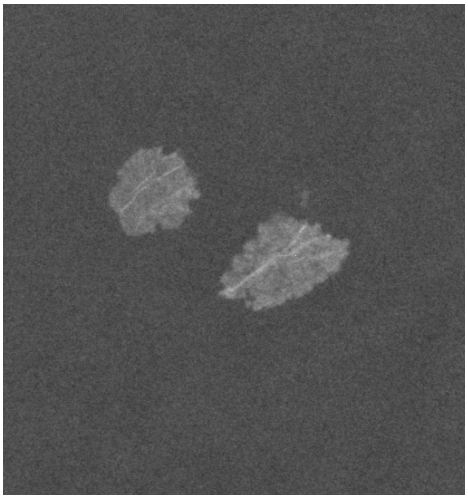

Figure 12. Subtracted image of iodine sample with BR3D material

4. Discussion

4.1 Detector response and uniformity

- Image pixel value and variance (standard deviation squared) were linear with mAs (and hence detector dose).
- Percentage non-uniformity measured using a raw high energy image of the contrast phantom was 1.1%. Only faint ghosting artefacts were seen.

4.2 Automatic exposure control

- Exposures in AEC mode were repeatable in terms of mAs, SD and CNR. Post exposure mAs values are consistent for CEM exposures.
- Exposure parameters (kV and filter) are different between low energy CEM exposures and standard 2D exposures due to the use of a different lookup table. Generally the MGD was higher for the low energy CEM, particularly for the 20 mm thick breasts.

4.3 Image subtraction

- For all iodine concentrations, the SD decreases with increasing phantom thickness when imaged in AEC mode; however the CNR remains relatively constant. The SD and CNR increase linearly with iodine concentration for any given phantom thickness.
- The system was able to successfully subtract the tissue-like structures in the BR3D material to reveal the iodine sample imaged.

4.4 Mean glandular dose

- The MGD for the 50 mm thick phantom was 1.03 mGy, 1.50 mGy and 0.54 mGy for the standard 2D, low energy contrast imaging exposure and high energy contrast imaging exposure respectively.
- The total MGD for a CEM exposure is approximately a third higher than the MGD of the low energy exposure alone for a 50 mm thick phantom.
- The maximum deviation between the indicated and calculated MGD was 15.4% for the low energy CEM exposure and 17.5% for the high energy CEM exposure, with a maximum error of 15.8% for the total MGD.

5. Conclusions

The system was found to be operating satisfactorily. Variations in SD and CNR with iodine concentration and phantom thickness follow similar trends to those seen in conference proceedings.[1,2] Different look up tables are used for the standard 2D and the low energy exposure; this can result in higher doses for the low energy exposure in particular for the 20 mm thick breasts.

References

1. Oduko, J., Homolka, P., Jones, V. and Whitwam, D. A Protocol for Quality Control Testing for Contrast-Enhanced Dual Energy Mammography Systems. In: Fujita H., Hara T. and Muramatsu C. eds. *IWDM 2014: Breast Imaging, 29 June – 2 July 2014,* Gifu City, Japan. Switzerland: Lecture Notes in Computer Science, Springer, Cham. 8539, pp. 407-414.

2. Oduko, J., Homolka, P., Jones, V. and Whitwam, D. Dose and Image Quality Measurements for Contrast-Enhanced Dual Energy Mammography Systems. Proceedings of SPIE, Medical Imaging 2015: Physics of Medical Imaging. Proceedings of SPIE. 2015, 9412, 94125I-1.

3. Young KC, Oduko JM, Gundogdu O and Asad M. *Technical evaluation of profile automatic exposure control software on GE Essential FFDM systems* (NHSBSP Equipment Report 0903). Sheffield: NHS Cancer Screening Programmes, 2009

4. Leithner R, Knogler T, Homolka P. Development and production of a prototype iodine contrast phantom for CEDEM, Physics in Medicine and Biology, 2013, 58, N25-35,

5. Dance, D.R., Skinner, C.L., Young, K.C., Beckett, J.R. and Kotre, C.J. Additional factors for the estimation of mean glandular breast dose using the UK mammography dosimetry protocol. Physics in Medicine and Biology. 2000, 45, pp. 3225–3240.

6 Kulama E, Burch A, Castellano I et al. *Commissioning and routine testing of full field digital mammography systems* (NHSBSP Equipment Report 0604, Version 3). Sheffield: NHS Cancer Screening Programmes, 2009

7. Dance, D.R. and Young, K.C. Estimation of mean glandular dose for contrast enhanced mammography: factors for use with the UK, European and IAEA breast dosimetry protocols. Physics in Medicine and Biology. 2014, 59, pp. 2127–2137.